Electronic Supplementary Material (ESI) for Journal of Materials Chemistry A.

Ultrafine platinum-iridium distorted nanowires as robust catalysts toward bifunctional hydrogen catalysis

Mingmin Wang[a], Mengjun Wang[a], Changhong Zhan[a], Hongbo Geng[c], Yunhua Li[a,*], Xiaoqing Huang[a,*], and Lingzheng Bu[b,*]

a. State Key Laboratory of Physical Chemistry of Solid Surfaces, College of Chemistry and Chemical Engineering, Xiamen University, Fujian, 361005, China.

b. College of Energy, Xiamen University, Fujian, 361102, China.

c. School of Materials Engineering, Changshu Institute of Technology, Jiangsu, 215500, China.

Experimental Procedures

1.1 Chemicals.

Platinum (II) acetylacetonate ($Pt(acac)_2$, 97%) and cetyltrimethylammonium bromide (CTAB, 98%) were purchased from Sigma-Aldrich. Iridium (III) acetylacetote ($Ir(acac)_3$, Ir, 38.0%-41.0%) was supplied by Tokyo Chemical Industry Co., LTD. Molybdenum hexacarbonyl ($Mo(CO)_6$, 98%) was purchased from Strem Chemicals Inc. Octadecenylamine ($C_{18}H_{37}N$, OAm) was supplied by Aladdin. Potassium hydrate (KOH, analytical reagent), cyclohexane (C_6H_{12}, analytical reagent, ≥99.7%), ethanol (C_2H_6O, analytical reagent, ≥99.7%) and isopropanol (C_3H_8O, analytical reagent, ≥99.7%) were purchased from Sinopharm Chemical Reagent Co. Ltd. Perchloric acid ($HClO_4$, analytical reagent, 70%-72%) was purchased from Tianjin Zhengcheng Chemical Products Co. Ltd. All chemical reagents were used as received without further purification. The deionized water with a resistivity of 18.2 MΩ cm^{-1} were prepared by passing water through an ultrapure purification system (Aqua Solutions).

1.2 Materials synthesis.

In a typical synthesis of Pt_2Ir DNWs, $Pt(acac)_2$ (10 mg), $Ir(acac)_3$ (6.2 mg), CTAB (90 mg), $Mo(CO)_6$ (15 mg), and 5 mL OAm were added into a glass vial (35 mL), followed by ultrasonication for 1 h. The homogeneous mixture was then heated from room temperature to 200 °C and maintained for 5 h in an oil bath. After cooling to room temperature, the products were collected via centrifugation and washed with ethanol and cyclohexane. The synthesis conditions of PtIr DNWs, Pt_4Ir DNWs, Pt_8Ir DNWs, and Pt DNWs were similar to those of Pt_2Ir DNWs except changing the amount of $Ir(acac)_3$ to 12.4, 3.1, 1.6, and 0 mg, respectively.

1.3 Preparation of carbon supported catalysts.

The as-synthesized nanowires were dispersed in cyclohexane (5 mL), and then mixed with commercial carbon support (C, Vulcan XC-72R) under ultrasonication for 0.5 h. After sonicating, the ethanol was added and sonicated for another 0.5 h. The product was collected by centrifugation and further washed twice with ethanol. Subsequently, the acetic acid and ethanol (v/v = 1/10) mixed solution was added and sonicated for 1 h. Finally, the acid-washed product was collected by centrifugation, washed with ethanol twice and dried under ambient condition to obtain the Pt-Ir DNWs/C with different compositions named as PtIr DNWs/C, Pt_2Ir DNWs/C, Pt_4Ir DNWs/C and Pt_8Ir DNWs/C, respectively. As a comparison, the Pt DNWs also loaded on the commercial carbon black, named as Pt DNWs/C. The loading amount of metals in these catalysts is 20% (wt.%), as determined by the inductively coupled

plasma optical emission spectroscopy (ICP-OES) and scanning electron microscope energy dispersive X-ray spectroscopy (SEM-EDS).

1.4 Characterization.

The transmission electron microscopy (TEM) samples were prepared by dropping cyclohexane or ethanol dispersion of samples on carbon-coated copper grids and dried under ambient condition. Low-magnification TEM was operated on JEM-1400 with an accelerating voltage of 100 kV. The high-resolution TEM (HRTEM) and scanning transmission electron microscopy (HAADF-STEM) was conducted on a FEI Tecnai F30 TEM at an accelerating voltage of 300 kV. X-ray diffraction (XRD) patterns were collected on a Smart Lab-SE powder diffractometer equipped with a Cu radiation source (λ = 0.15406 nm). SEM-EDS was taken by ZEISS Sigma 300 field emission scanning electron microscope. The X-ray photoelectron spectroscopy spectra (XPS) were collected by XPS (Thermo Scientific, ESCALAB 250 XI). The carbon peak at 284.8 eV was used as the reference to correct for charging effects. The concentration of catalysts was determined by the ICP-OES (ICAP 7000, Thermo Fisher Scientific, Waltham, MA USA).

1.5 Electrochemical measurements.

All the electrochemical measurements were carried out on a CHI 660E electrochemical workstation (CH Instruments, Chenhua Co., Shanghai, China). A three-electrode cell was used to perform the electrochemical measurements. The glass carbon electrode, leak-free saturated calomel electrode (SCE) and graphite rod were served as the working electrode, reference electrode and counter electrode, respectively. All potentials were measured against the reversible hydrogen electrode (RHE) by $E(RHE) = E(vs\ SCE) + 0.24V + 0.0591 \times pH$ through the calibration of SCE. The catalyst ink was prepared by mixing 2 mg catalysts and 5 μL Nafion (5%, wt.%) with 1 mL isopropanol and sonicated for 1 h. Then 5 μL suspension (10.20 μg cm^{-2} metals) was deposited on a glassy carbon electrode/rotating disk electrode (RDE) (0.196 cm^2) to obtain the working electrodes for HER/HOR, respectively.

At the beginning of measurement, the catalysts were cycled about 100 times of cyclic voltammograms (CVs) at 500 mV s^{-1} between -0.25 V and 1 V until achieving a stable CV curve. Then the CVs at 50 mV s^{-1} was then applied to determine the ECSAs of catalysts according to the underpotentially deposited H (H_{upd}) methods.

HER measurements were performed in Ar-saturated 0.1 M KOH electrolyte with 90% IR compensation. The linear sweep voltammetry (LSV) was conducted at the scan rate of 5 mV s^{-1}. The current densities

were normalized to the geometric area of the working electrode. The accelerated durability test was carried out at room temperature between -0.1 V and 0.4 V in 0.1 M KOH at the scan rate of 500 mV s^{-1}. HOR measurements were performed in H_2-saturated 0.1 M KOH electroyte by a RDE system. The HOR polarization curves were conducted at the scan rate of 5 mV s^{-1} with the rotating speed of 1600 rpm. The scan rate of different rotating rates (400, 900, 1600 and 2500 rpm) was also 5 mV s^{-1}. The durability of different catalysts was also evaluated by applying chronoamperometry test at 100 mV in H_2-saturated 0.1 M KOH. The accelerated durability test was carried out at room temperature between -0.1 V and 0.4 V in 0.1 M KOH at the scan rate of 500 mV s^{-1}. The anti-CO poisoning ability test was carried out in 0.1 M KOH purged with saturated 100 ppm CO/H_2. The current-time chronoamperometry test was performed at 100 mV.

The kinetic current (j_k) was calculated with the Koutecky-Levich equation.

$$\frac{1}{j} = \frac{1}{j_k} + \frac{1}{j_d} \tag{1}$$

where the measured current (j) can be divided into kinetic current (j_k) and diffusion limited current (j_d) which follow the Butler-Volmer equation and Levich equation, respectively.

$$j_k = j_0(e^{\frac{\alpha_a F \eta}{RT}} - e^{-\frac{\alpha_c F \eta}{RT}}) \tag{2}$$

$$j_d = BC_0\omega^{1/2} \tag{3}$$

in which α_a and α_c are the anodic and cathodic transfer coefficients (α_a + α_c = 1), F is the Faraday constant, η is the overpotential, R is the universal gas constant, T is the Kelvin temperature, B is the Levich constant kinetic, C_0 is the solubility of H_2 in KOH electrolyte, and ω is the rotating speed.

For CO-stripping measurements, the catalysts was subjected to 200 cycles of potential sweeps at 500 mV s^{-1} in 0.1 M $HClO_4$ and then the CO gas was bubbled in the solution for 20 min. After that, the electrode was quickly moved to a fresh solution and record the CV curves at the rate of 20 mV s^{-1} without additional CO introduction.

Supporting Figures

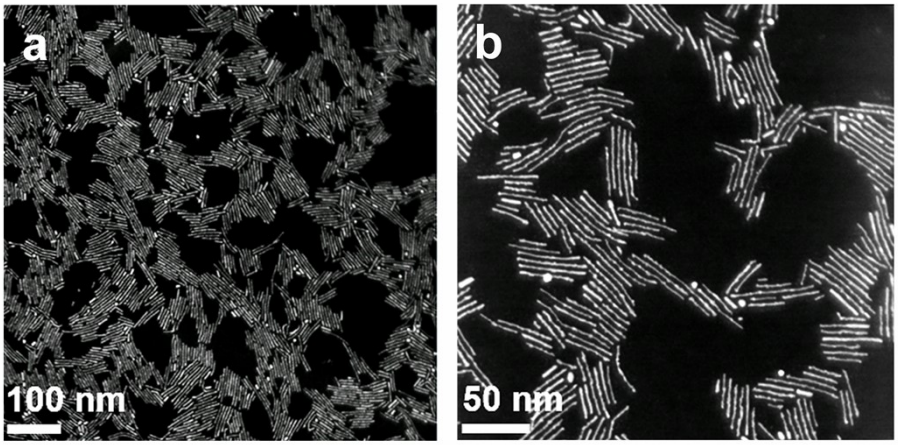

Figure S1. (**a**, **b**) HAADF-STEM images of Pt_2Ir DNWs.

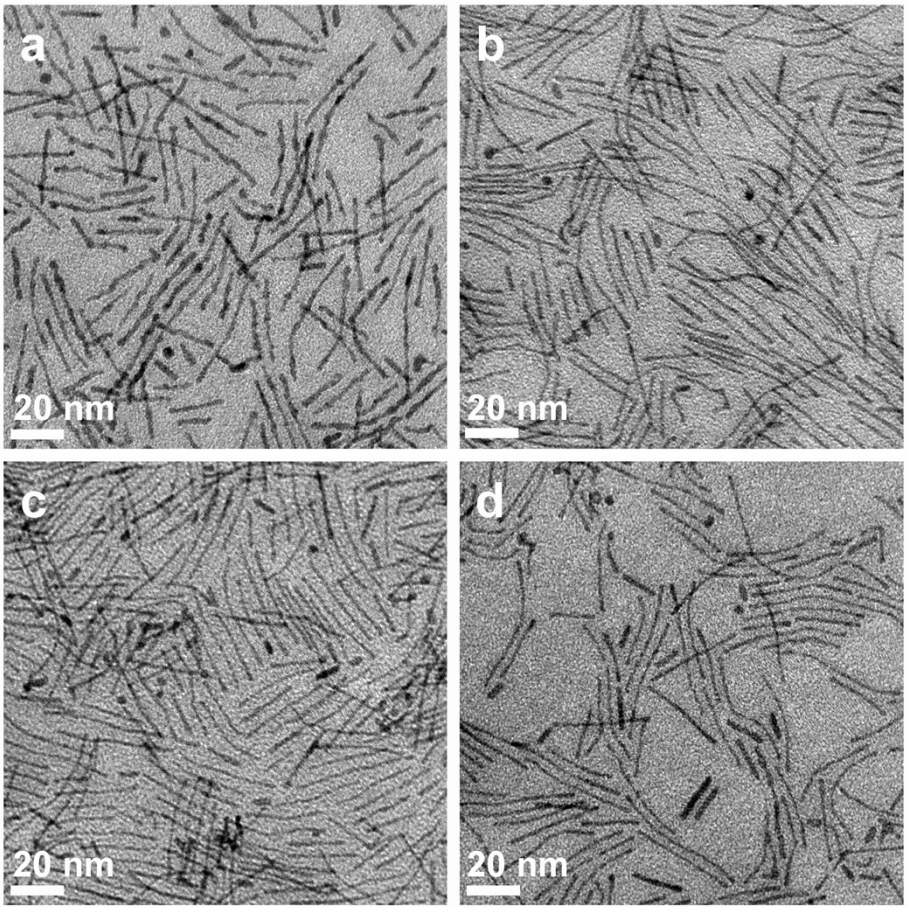

Figure S2. TEM images of (**a**) PtIr DNWs, (**b**) Pt_4Ir DNWs, (**c**) Pt_8Ir DNWs, and (**d**) Pt DNWs.

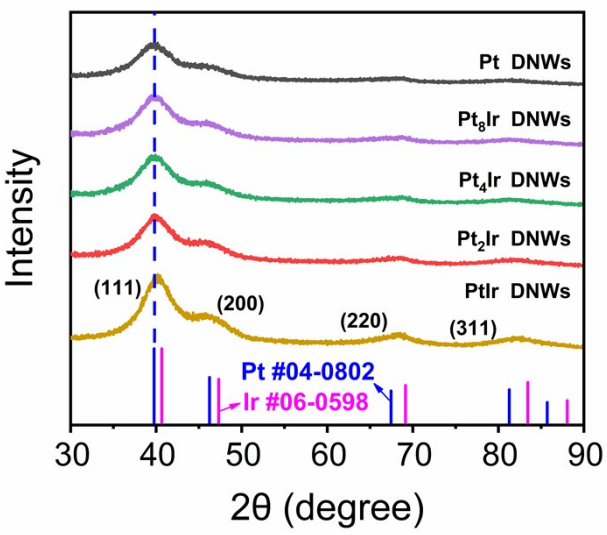

Figure S3. XRD patterns of PtIr DNWs, Pt_2Ir DNWs, Pt_4Ir DNWs, Pt_8Ir DNWs, and Pt DNWs.

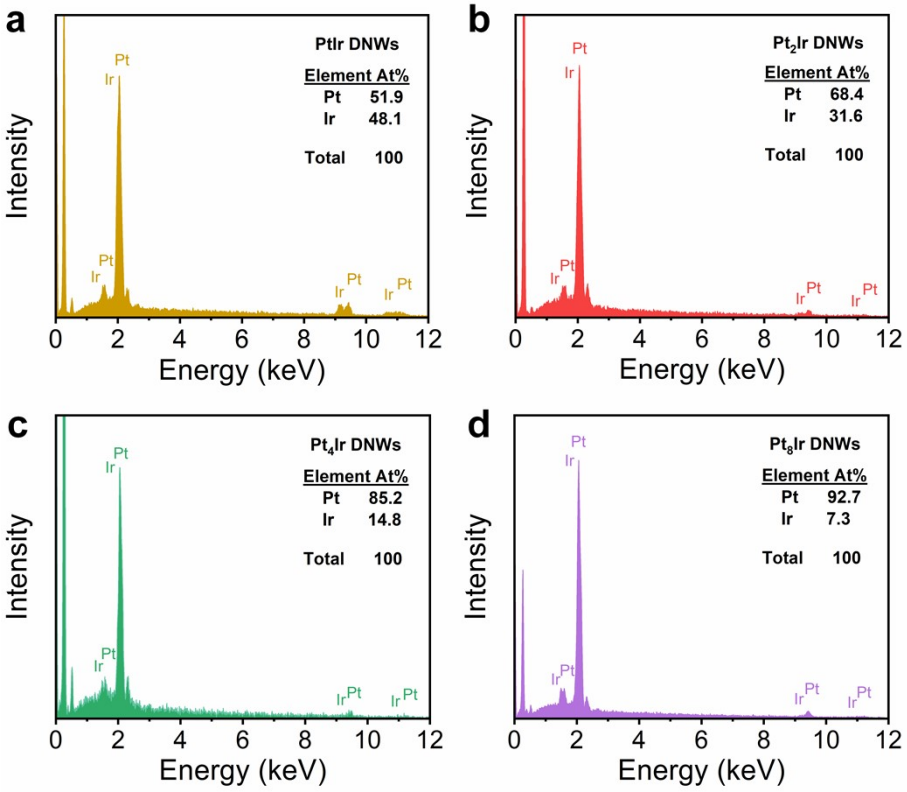

Figure S4. SEM-EDS patterns of (**a**) PtIr DNWs, (**b**) Pt_2Ir DNWs, (**c**) Pt_4Ir DNWs, and (**d**) Pt_8Ir DNWs.

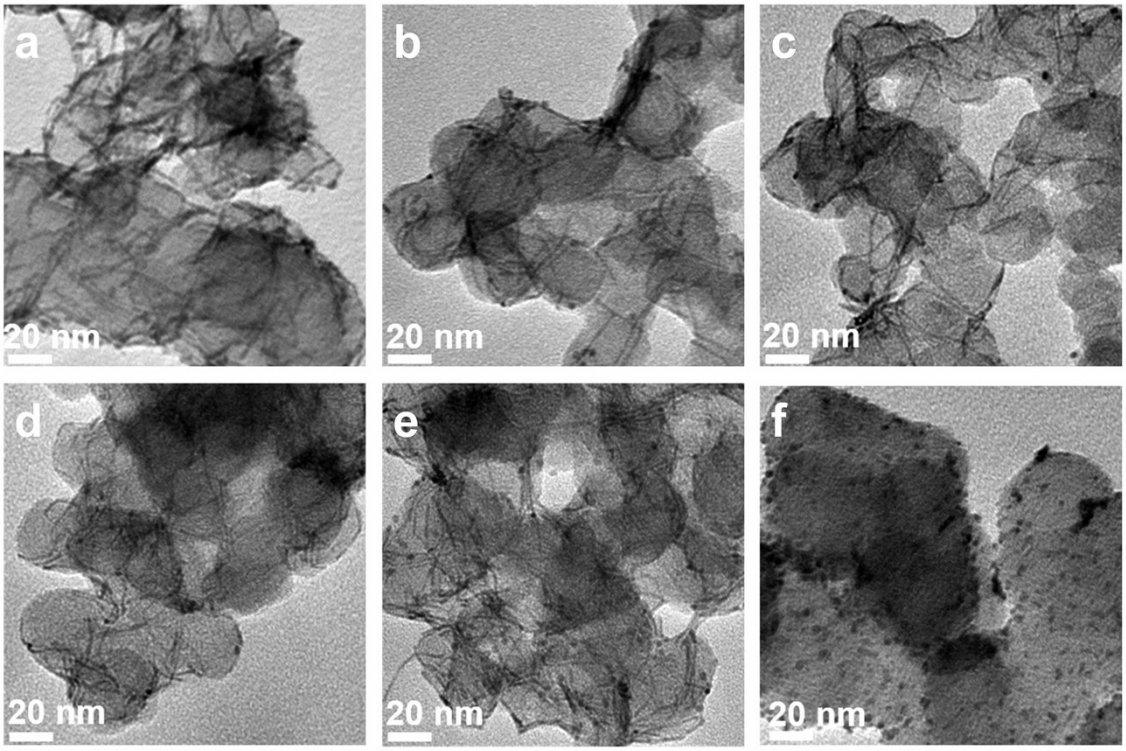

Figure S5. TEM images of (**a**) PtIr DNWs/C, (**b**) Pt_2Ir DNWs/C, (**c**) Pt_4Ir DNWs/C, (**d**) Pt_8Ir DNWs/C, (**e**) Pt DNWs/C, and (**f**) commercial Pt/C.

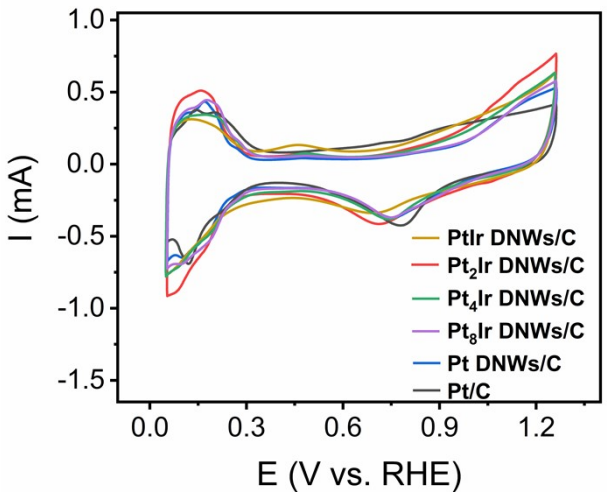

Figure S6. CVs of different catalysts in 0.1 M $HClO_4$ at the scan rate of 50 mV s^{-1}.

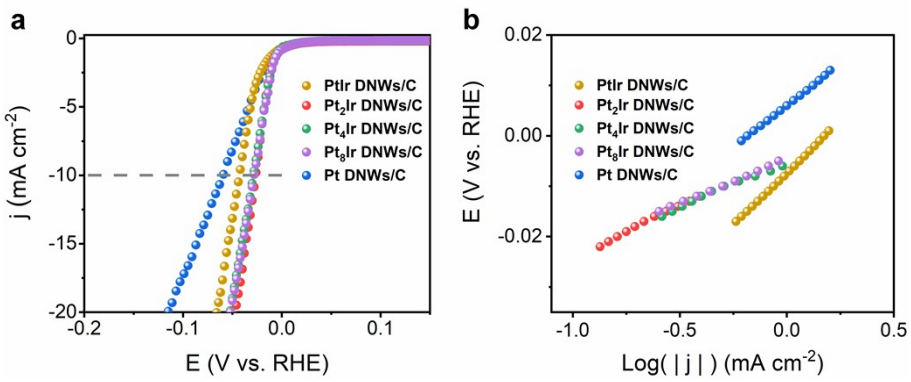

Figure S7. (**a**) HER polarization curves and (**b**) Tafel plots of different catalysts.

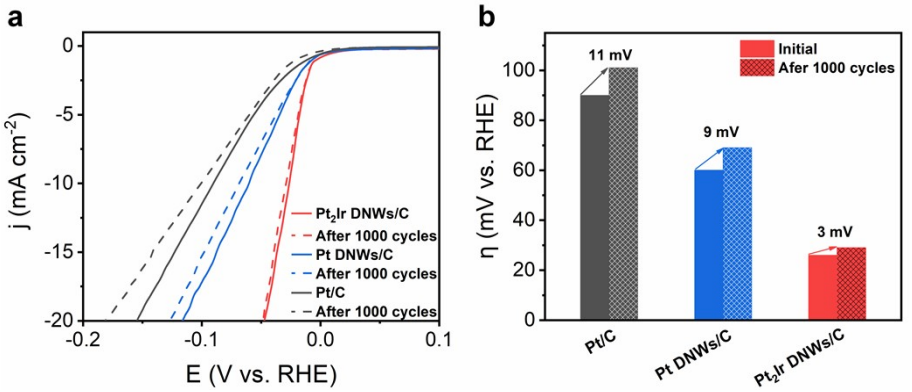

Figure S8. (**a**) HER polarization curves and (**b**) histograms of comparative overpotentials for different catalysts before and after stability test.

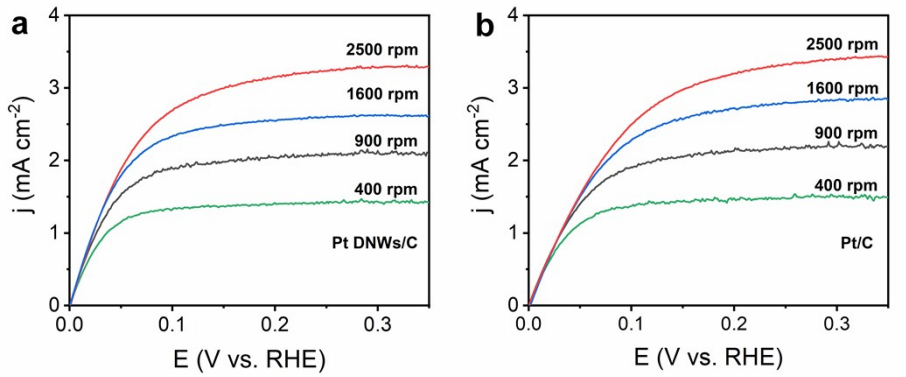

Figure S9. HOR polarization curves of (**a**) Pt DNWs/C and (**b**) Pt/C at the rotating speeds varied from 400 to 2500 rpm.

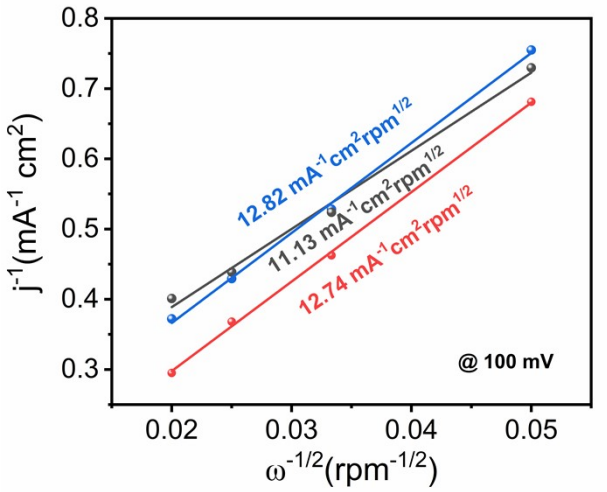

Figure S10. Koutecky-Levich plots of different catalysts at the overpotential of 100 mV.

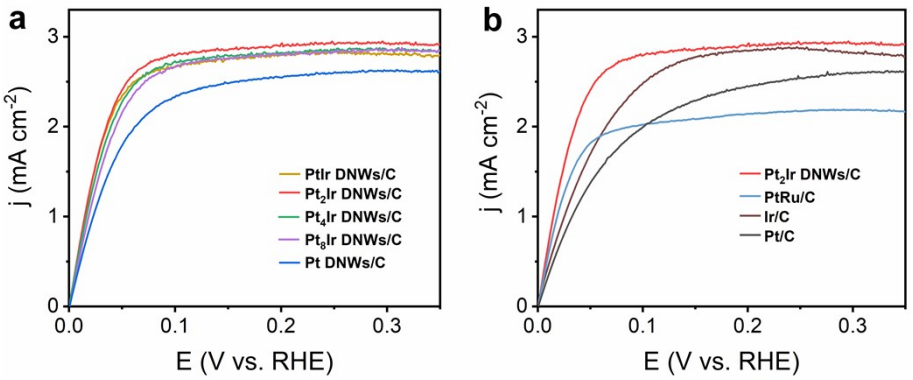

Figure S11. (**a**) HOR polarization curves of different Pt-Ir DNWs/C and Pt DNWs/C. (**b**) HOR polarization curves of Pt_2Ir DNWs/C and commercial catalysts.

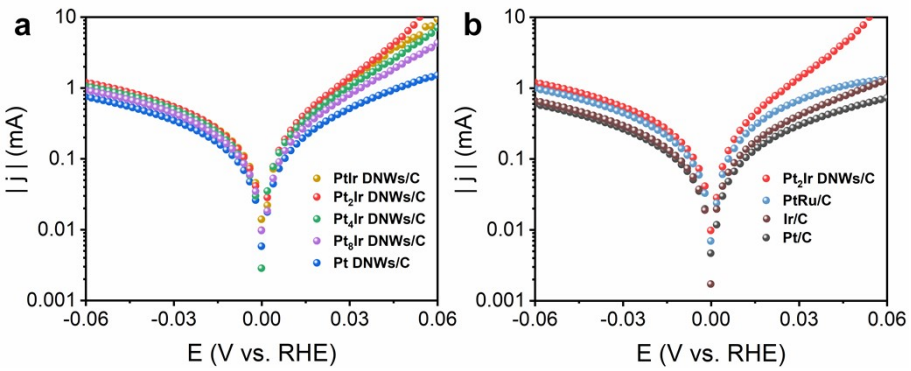

Figure S12. (**a**) Tafel plots of different Pt-Ir DNWs/C and Pt DNWs/C. (**b**) Tafel plots of Pt_2Ir DNWs/C and commercial catalysts.

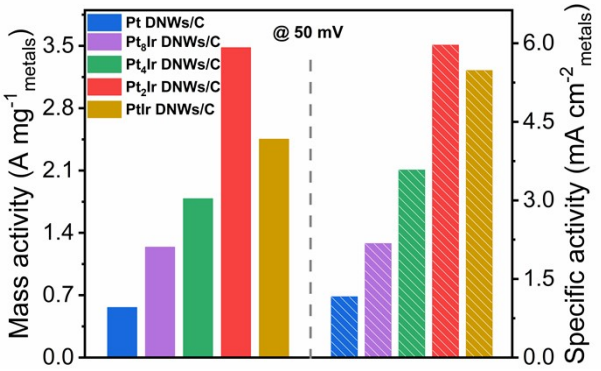

Figure S13. ECSA-normalized specific activities and mass activities of different catalysts at 50 mV.

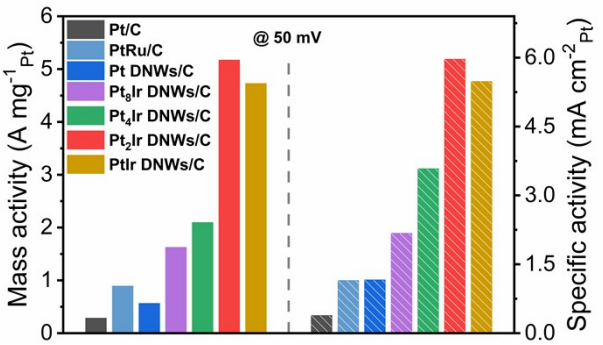

Figure S14. Specific activities and Pt-normalized mass activities of different catalysts at 50 mV.

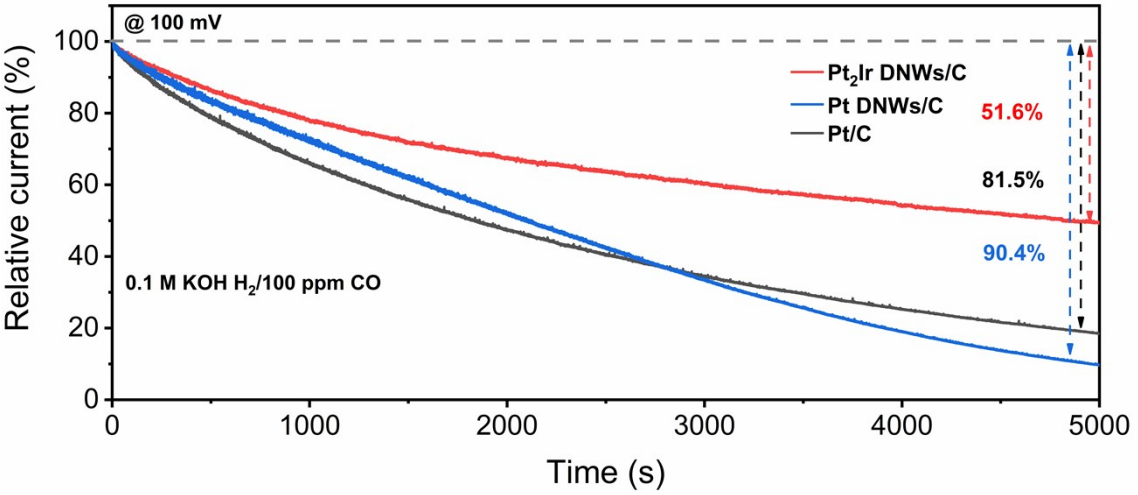

Figure S15. Relative current-time chronoamperometry responses of Pt_2Ir DNWs/C, Pt DNWs/C, and commercial Pt/C in H_2/100 ppm CO-saturated 0.1 M KOH solution at 100 mV.

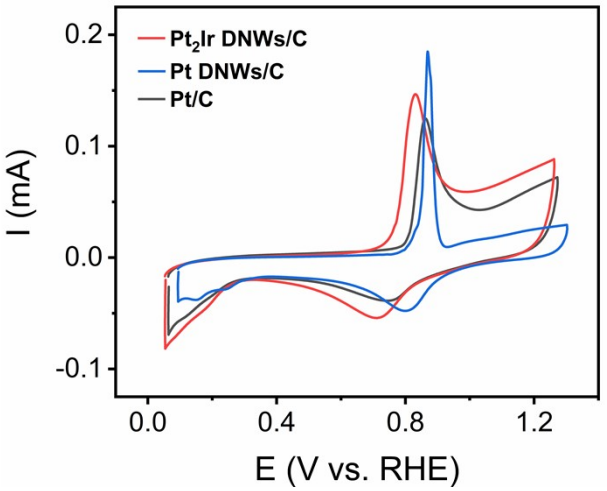

Figure S16. CO-stripping curves of different catalysts after 2000 cycles accelerated durability test in 0.1 M HClO4 solution at a scan rate of 20 mV s^{-1}.

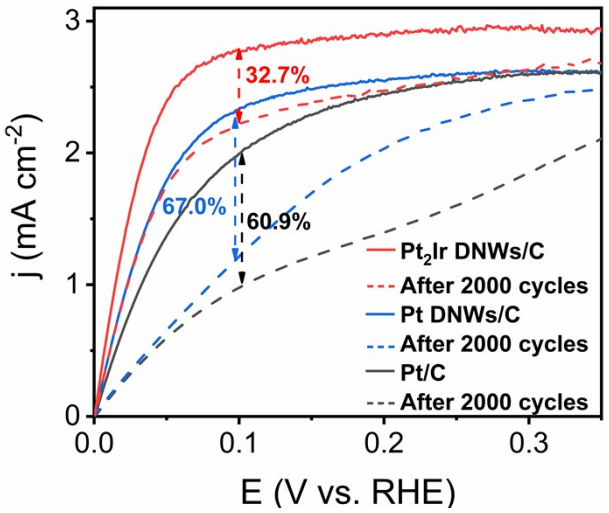

Figure S17. HOR polarization curves of Pt_2Ir DNWs/C, Pt DNWs/C and commercial Pt/C in H_2-saturated 0.1 M KOH before (solid line) and after (dashed line) 2000 cycles.

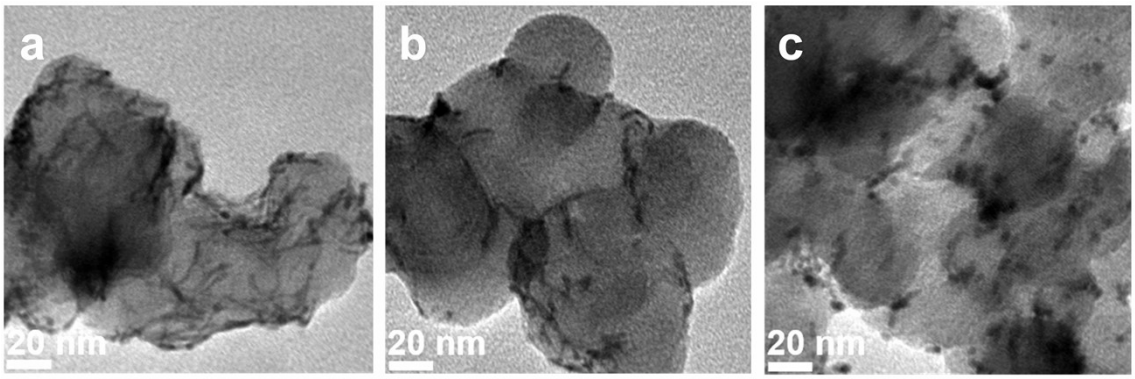

Figure S18. TEM images of (**a**) Pt_2Ir DNWs/C, (**b**) Pt DNWs/C, and (**c**) commercial Pt/C after the current-time chronoamperometry test.

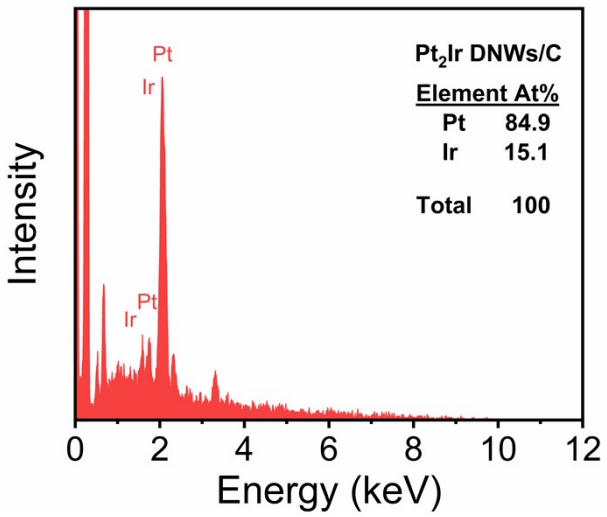

Figure S19. SEM-EDS pattern of Pt_2Ir DNWs/C after the current-time chronoamperometry test.

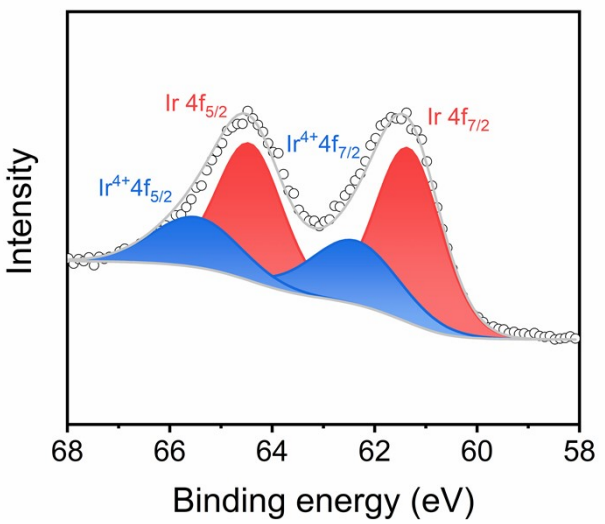

Figure S20. Ir 4f XPS spectrum of Pt_2Ir DNWs/C.

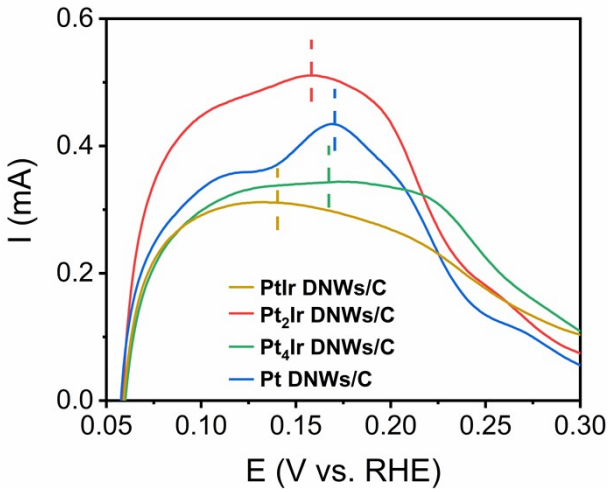

Figure S21. The H_{upd} electrochemical desorption curves of PtIr DNWs/C, Pt_2Ir DNWs/C, Pt_4Ir DNWs/C, and Pt DNWs/C in 0.1 M $HClO_4$.

Supporting Tables

Table S1. The loading amounts and ECSAs of different catalysts.

Catalyst	Loading (μg_{metals} cm^{-2})	Loading (μg_{Pt} cm^{-2})	ECSA (m^2 $gmetals^{-1}$)	ECSA (m^2 g_{Pt}^{-1})
PtIr DNWs/C	10.20	5.31	44.77	86.26
Pt_2Ir DNWs/C	10.20	6.89	58.35	86.68
Pt_4Ir DNWs/C	10.20	8.67	49.84	58.49
Pt_8Ir DNWs/C	10.20	9.44	56.97	61.69
Pt DNWs/C	10.20	10.20	48.46	48.46
Pt/C	10.20	10.20	74.04	74.04
Ir/C	10.20	/	36.70	/
PtRu/C	10.20	6.80	34.47	51.70

Table S2. Summary of the reported Pt-based catalysts for alkaline HER.

Catalyst	Electrolyte	Overpotential @10 mA cm^{-2} (mV)	Tafel slope ($mV \cdot dec^{-1}$)	Ref.
Pt_2Ir DNWs/C	**0.1 M KOH**	**26**	**20.9**	**This work**
Ni $(OH)_2$/Pt/C (TTK)	0.1 M KOH	~90	~110	*1*
Pt_2Ni_3-P NWs	0.1 M KOH	68	66	*2*
Pt NWs/SL-Ni $(OH)_2$	0.1 M KOH	~48	-	*3*
Pt_3Ni_2-NWs-S/C	0.1 M KOH	45	-	*4*
Pt(pc) electrode	0.1 M KOH	-	113	*5*
Pt/NiRu-OH	1 M KOH	38	39	*6*
α-MoC_{1-x}/Pt nanoparticles	1 M KOH	67	55	*7*

Table S3. The mass activities (j_m), specific activities (j_s), and exchange current (j_0) at 50 mV of different catalysts

Catalyst	j_m, 50 mV ($A\ mg_{metals}^{-1}$)	j_m, 50 mV ($A\ mg_{Pt}^{-1}$)	j_s, 50 mV ($mA\ cm^{-2}$)	j_0 (mA)	α
PtIr DNWs/C	2.45	4.73	5.48	0.72	0.96
Pt_2Ir DNWs/C	**3.48**	**5.17**	**5.96**	**0.71**	**0.92**
Pt_4Ir DNWs/C	1.78	2.09	3.58	0.62	0.88
Pt_8Ir DNWs/C	1.24	1.62	2.17	0.51	0.81
Pt DNWs/C	0.56	0.56	1.16	0.35	0.66
Pt/C	0.28	0.28	0.38	0.23	0.55
Ir/C	0.46	/	1.26	0.27	0.65
PtRu/C	0.59	0.89	1.15	0.40	0.56

Table S4 Summary of the reported Pt-based catalysts for alkaline HOR.

Catalyst	Electrolyte	j_m, 50 mV (A mg_{metals}^{-1})	j_s, 50 mV (mA cm^{-2})	Ref.
Pt_2Ir DNWs/C	**0.1 M KOH**	**3.48**	**5.96**	**This work**
Pt/NiO	0.1 M KOH	~ 0.2	8.10	*8*
core–shell Pt_3Co	0.1 M KOH	0.24	1.43	*9*
$Ru_{0.90}Pt_{0.10}$ NTs	0.1 M KOH	0.24	2.43	*10*
$(Pt_{0.9}Pd_{0.1})_3Fe$/C	0.1 M KOH	0.31	0.99	*11*
$Pt_{0.9}Pd_{0.1}$/C	0.1 M KOH	0.26	0.73	*11*
PtNi/C	0.1 M KOH	0.32	1.55	*12*
Acid treated PtNi/C	0.1 M KOH	0.47	1.89	*12*
PtFe NWs	0.1 M KOH	0.46	1.68	*13*
PtRu NWs	0.1 M KOH	0.60	2.20	*13*
PtCu NWs	0.1 M KOH	0.65	2.10	*13*
Pt-(PtO_x)-NSs/C	0.1 M KOH	0.50	-	*14*
Pd_3Fe@Pt/C	0.1 M KOH	0.66	0.52	*15*
Pd_3Co@Pt/C	0.1 M KOH	0.69	0.57	*15*
Ru@Pt NPs	1 M KOH	1.03	-	*16*
PtNb/NbO_x/C	0.1 M KOH	1.80	-	*17*
Mo-Pt/NC	0.1 M KOH	4.54	25 mV @ ~ 4.40	*18*

Reference

1. R. Subbaraman, D. Tripkovic, D. Strmcnik, K. C. Chang, M. Uchimura, A. P. Paulikas, V. Stamenkovic and N. M. Markovic, *Science*, 2011, **334**, 1256-1260.
2. P. Wang, Q. Shao, J. Guo, L. Bu and X. Huang, *Chem. Mater.*, 2020, **32**, 3144-3149.
3. H. Yin, S. Zhao, K. Zhao, A. Muqsit, H. Tang, L. Chang, H. Zhao, Y. Gao and Z. Tang, *Nat. Commun.*, 2015, **6**, 6430.
4. P. Wang, X. Zhang, J. Zhang, S. Wan, S. Guo, G. Lu, J. Yao and X. Huang, *Nat. Commun.*, 2017, **8**, 14580.
5. W. Sheng, M. Myint, J. G. Chen and Y. Yan, *Energy Environ. Sci.*, 2013, **6**, 1509.
6. D. Li, X. Chen, Y. Lv, G. Zhang, Y. Huang, W. Liu, Y. Li, R. Chen, C. Nuckolls and H. Ni, *Appl. Catal. B*, 2020, **269**, 118824.
7. H. J. Song, M. C. Sung, H. Yoon, B. Ju and D. W. Kim, *Adv. Sci.,* 2019, **6**, 1802135.
8. G. Zhao, L. Xia, P. Cui, Y. Qian, Y. Jiang, Y. Zhao, H. Pan, S. X. Dou and W. Sun, *Nano Lett.*, 2021, **21**, 4845-4852.
9. D. J. Weber, C. Dosche and M. Oezaslan, *J. Mater. Chem. A*, 2021, **9**, 15415-15431.
10. S. St. John, R. W. Atkinson, K. A. Unocic, R. R. Unocic, T. A. Zawodzinski and A. B. Papandrew, *ACS Catal.*, 2015, **5**, 7015-7023.
11. T. Zhao, G. Wang, M. Gong, D. Xiao, Y. Chen, T. Shen, Y. Lu, J. Zhang, H. Xin, Q. Li and D. Wang, *ACS Catal.*, 2020, **10**, 15207-15216.
12. S. Lu and Z. Zhuang, *J. Am. Chem. Soc.*, 2017, **139**, 5156-5163.
13. M. E. Scofield, Y. Zhou, S. Yue, L. Wang, D. Su, X. Tong, M. B. Vukmirovic, R. R. Adzic and S. S. Wong, *ACS Catal.*, 2016, **6**, 3895-3908.
14. M. K. Kundu, T. Bhowmik, R. Mishra and S. Barman, *ChemSusChem*, 2018, **11**, 2388-2401.
15. T. Zhao, Y. Hu, M. Gong, R. Lin, S. Deng, Y. Lu, X. Liu, Y. Chen, T. Shen, Y. Hu, L. Han, H. Xin, S. Chen and D. Wang, *Nano Energy*, 2020, **74**, 104877.
16. K. Elbert, J. Hu, Z. Ma, Y. Zhang, G. Chen, W. An, P. Liu, H. S. Isaacs, R. R. Adzic and J. X. Wang, *ACS Catal.*, 2015, **5**, 6764-6772.
17. S. Ghoshal, Q. Jia, M. K. Bates, J. Li, C. Xu, K. Gath, J. Yang, J. Waldecker, H. Che, W. Liang, G. Meng, Z.-

F. Ma and S. Mukerjee, *ACS Catal.*, 2017, **7**, 4936-4946.

18. M. Ma, G. Li, W. Yan, Z. Z. Wu, Z. P. Zheng, X. B. Zhang, Q. X. Wang, G. F. Du, D. Y. Liu, Z. X. Xie, Q. Kuang and L. S. Zheng, *Adv. Energy Mater.*, 2022, **12**, 2103336.